In vivo generated hematopoietic stem cells from genome edited induced pluripotent stem cells are functional in platelet-targeted gene therapy of murine hemophilia A

Dawei Wang,[1,2] Guowei Zhang,[1,3] Junjie Gu,[4] Xiaohu Shao,[1] Yuting Dai,[1] Jianfeng Li,[1] Xiaohong Pan,[1] Shuxian Yao,[1] Aining Xu,[1] Ying Jin,[4] Jinyan Huang,[1] Qizhen Shi,[5] Jiang Zhu,[1] Xiaodong Xi,[1] Zhu Chen[1,2] and Saijuan Chen[1,2]

[1]*State Key Laboratory of Medical Genomics, Shanghai Institute of Hematology, Ruijin Hospital Affiliated to Shanghai Jiao Tong University School of Medicine, Shanghai, China;* [2]*National Research Center for Translational Medicine, Shanghai Jiao Tong University School of Medicine, Shanghai, China;* [3]*Key Laboratory of Aging and Cancer Biology of Zhejiang Province, Hangzhou Normal University School of Medicine, Hangzhou, China;* [4]*Key Laboratory of Stem Cell Biology, Center for The Excellence in Molecular and Cell Sciences, Institute of Health Sciences, Shanghai Institutes for Biological Sciences, Chinese Academy of Sciences and Shanghai Jiao Tong University School of Medicine, Shanghai, China and* [5]*Department of Pediatrics, Medical College of Wisconsin, Milwaukee, WI, USA*

Correspondence: SAIJUAN CHEN - sjchen@stn.sh.cn or GUOWEI ZHANG - gzhang@hznu.edu.cn

doi:10.3324/haematol.2019.219089

Supplementary Materials

In vivo generated hematopoietic stem cells from genome edited induced pluripotent stem cells are functional in platelet-targeted gene therapy of murine hemophilia A

Dawei Wang[1,2], Guowei Zhang[1,3,*], Junjie Gu[4], Xiaohu Shao[1], Yuting Dai[1], Jianfeng Li[1], Xiaohong Pan[1], Shuxian Yao[1], Aining Xu[1], Ying Jin[4], Jinyan Huang[1], Qizhen Shi[5], Jiang Zhu[1,2], Xiaodong Xi[1], Zhu Chen[1,2] and Saijuan Chen[1,2,*]

[1]State Key Laboratory of Medical Genomics, Shanghai Institute of Hematology, Ruijin Hospital Affiliated to Shanghai Jiao Tong University School of Medicine, Shanghai, China;

[2]The National Research Center for Translational Medicine, Shanghai Jiao Tong University School of Medicine, Shanghai, China;

[3]School of Medicine, Hangzhou Normal University, Hangzhou, China;

[4]Key Laboratory of Stem Cell Biology, Center for The Excellence in Molecular and Cell Sciences, Institute of Health Sciences, Shanghai Institutes for Biological Sciences, Chinese Academy of Sciences and Shanghai Jiao Tong University School of Medicine, Shanghai, China;

[5]Department of Pediatrics, Medical College of Wisconsin, Milwaukee, MI, USA

Twelve supplemental figures

Six supplemental tables

Materials and methods

Supplemental figures

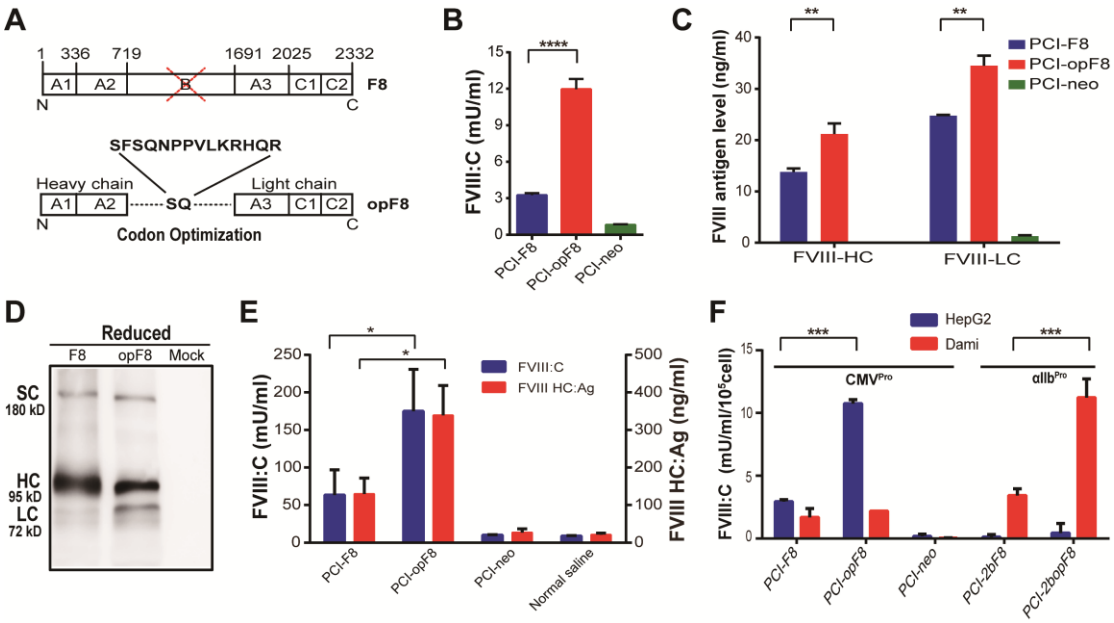

Figure S1. Tests of the Codon-optimized FVIII.

(A) Schematic of the codon-optimized FVIII. B domain was replaced by the SQ sequence in the codon-optimized FVIII. F8 and opF8 represent B domain deleted FVIII and codon-optimized FVIII, respectively. (B) and (C) FVIII expression in HEK293T cells, which were transfected by PCI-F8, PCI-opF8, and PCI-neo (mock vector). Supernatants were collected for FVIII:C (B) and FVIII antigen (C) analysis. The FVIII:C level of opF8 was about 3.7-fold of that of F8, and antigen levels of HC and LC were significantly higher in the opF8 group than those in the F8 group. The results were representative of three independent experiments. PCI-F8 and PCI-opF8 represent CMV promoter controlled F8 and opF8 cassette, respectively. (D) Western blot analysis of FVIII expressed in HEK293T cells. For both samples, HC and LC of FVIII were displayed in the bands of expected molecular weight. HC and LC represent heavy chain and light chain of FVIII, respectively. (E) Plasma FVIII level of the hydrodynamically injected HA mice. Plasma was collected 24 hours after hydrodynamic injection. FVIII:C and HC antigen were detected at higher levels in the opF8 group. (F) Determination of FVIII expression under αIIb promoter, the megakaryocyte/platelet specific promoter, in Dami cells and HepG2 cells.

FVIII:C of opF8-transfected cells was significantly higher than that of F8-transfected cells for either αIIb or CMV promoter controlled cassettes. 2bopF8 and 2bF8 were expressed in Dami cells but not in HepG2 cells, proving the specificity of αIIb promoter. PCI-2bF8 and PCI-2bopF8 represent αIIb promoter controlled F8 and opF8 cassette, respectively. The results were representative of three independent experiments. Mean ± SD values are shown. *P < .05, **P < .01, ***P < .001, ****P < .0001.

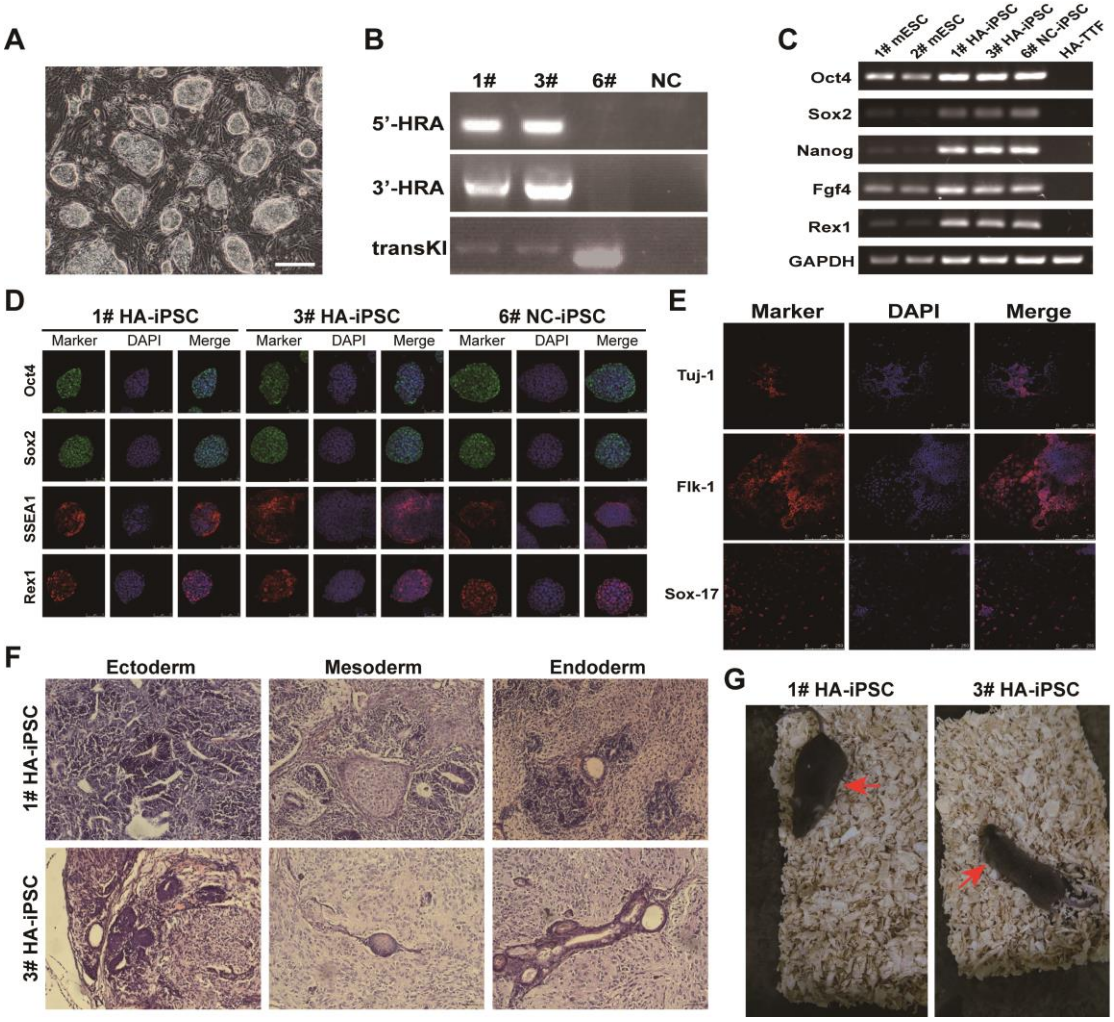

Figure S2. Pluripotent stem cell features and FVIII genotype of HA-iPSCs.

(A) Representative image of HA-iPSCs. Scale bar, 50 μm. (B) Genotyping analysis of HA-iPSCs (1# and 3#) and NC-iPSCs (6#). FVIII knockout feature was shown in HA-iPSCs. HRA, homologous arm; transKI, the replaced region of FVIII. NC-iPSCs represent wild-type mouse iPSCs. (C) RT-PCR analysis of the expression of pluripotency marker genes in HA-iPSCs. The endogenous pluripotent genes *Nanog*, *Fgf4*, *Rex1* and activated genes *Oct4*, *Sox2* were expressed in HA-iPSCs but undetected in HA mouse tail tip fibroblasts (HA-TTFs). (D) Immunostaining of HA-iPSCs (1# and 3#) and NC-iPSCs (6#) for cell surface markers, including Oct-4, Sox-2, SSEA1 and Rex1. The cells are positive for these markers. Scale bar, 75 μm. (E) Immunofluorescence staining of *in vitro* differentiated cells from the embryoid bodies (EBs) formed by HA-iPSCs by using antibodies against Sox17 (endoderm marker), Flk1

(mesoderm marker) and Tuj1 (ectoderm marker). All markers of the three germ layers were expressed in the cells. Scale bar, 50 μm. (F) HE staining of teratoma sections. Teratoma was formed 4 weeks after injection of HA-iPSCs into NOD-SCID mice, and tissues from all three types of germ layers were observed. Respiratory epithelium (endoderm), cartilage (mesoderm), and neural epithelium (ectoderm) are shown. Scale bar, 50 μm. (G) The potential of the established HA-iPSCs for ontogeny was confirmed by blastocyst injection to generate chimeric mice.

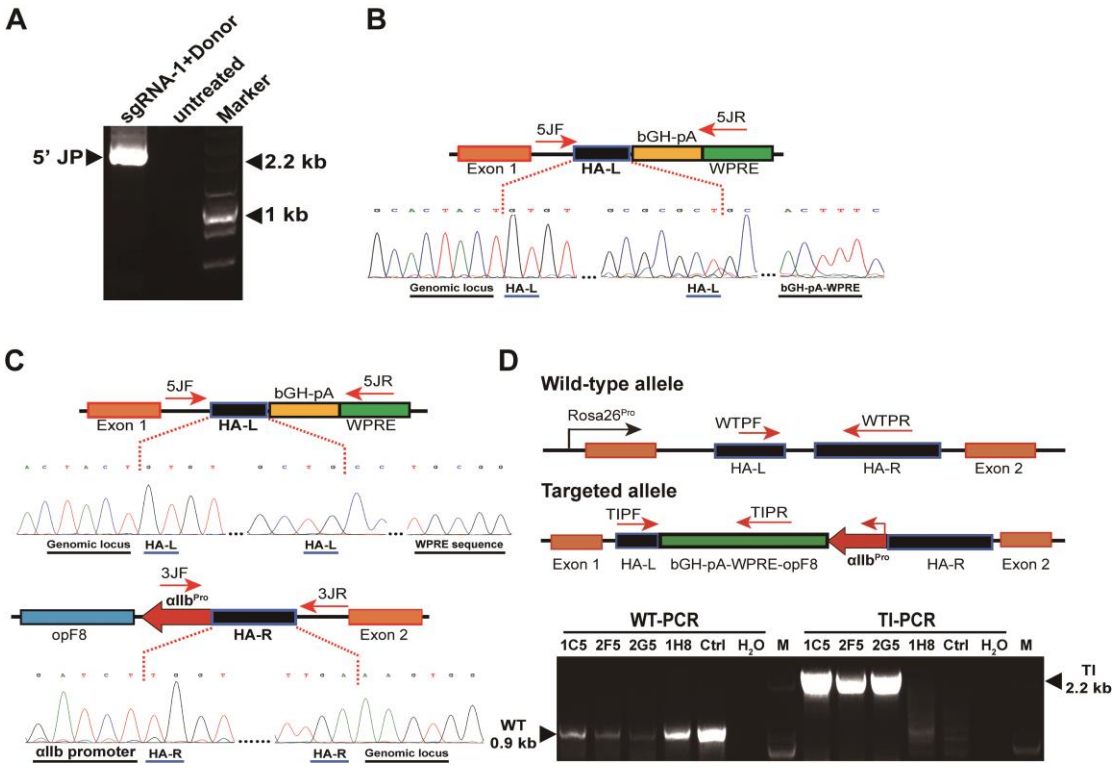

Figure S3. Analysis of 2bopF8 target integration in 3T3 cells and 2bopF8-HAiPSCs.

(A) Co-transfection of the Cas9/sgRNA-1 plasmid and the 2bopF8 donor plasmid into 3T3 cells, and the representative 5'-junction PCR product was verified. (B) DNA sequencing result of the 5'-junction PCR product acquired in (A), indicating that the 2bopF8 cassette was successfully integrated into the target site in the 3T3 Rosa26 locus. (C) Sequencing results of the 5'- and 3'-junction PCR products of 2bopF8-HAiPSCs, showing correct integration of 2bopF8 at the Rosa26 locus. (D) Determination of the genotype of 2bopF8-HAiPSCs by allele-specific PCR. Allele-specific PCR primers are shown in red arrows. PCR products corresponding to the WT (0.9 kb) and the inserted gene (2 kb) were amplified in the three clones, revealing that the three 2bopF8-HAiPSC clones contain single copy of 2bopF8.

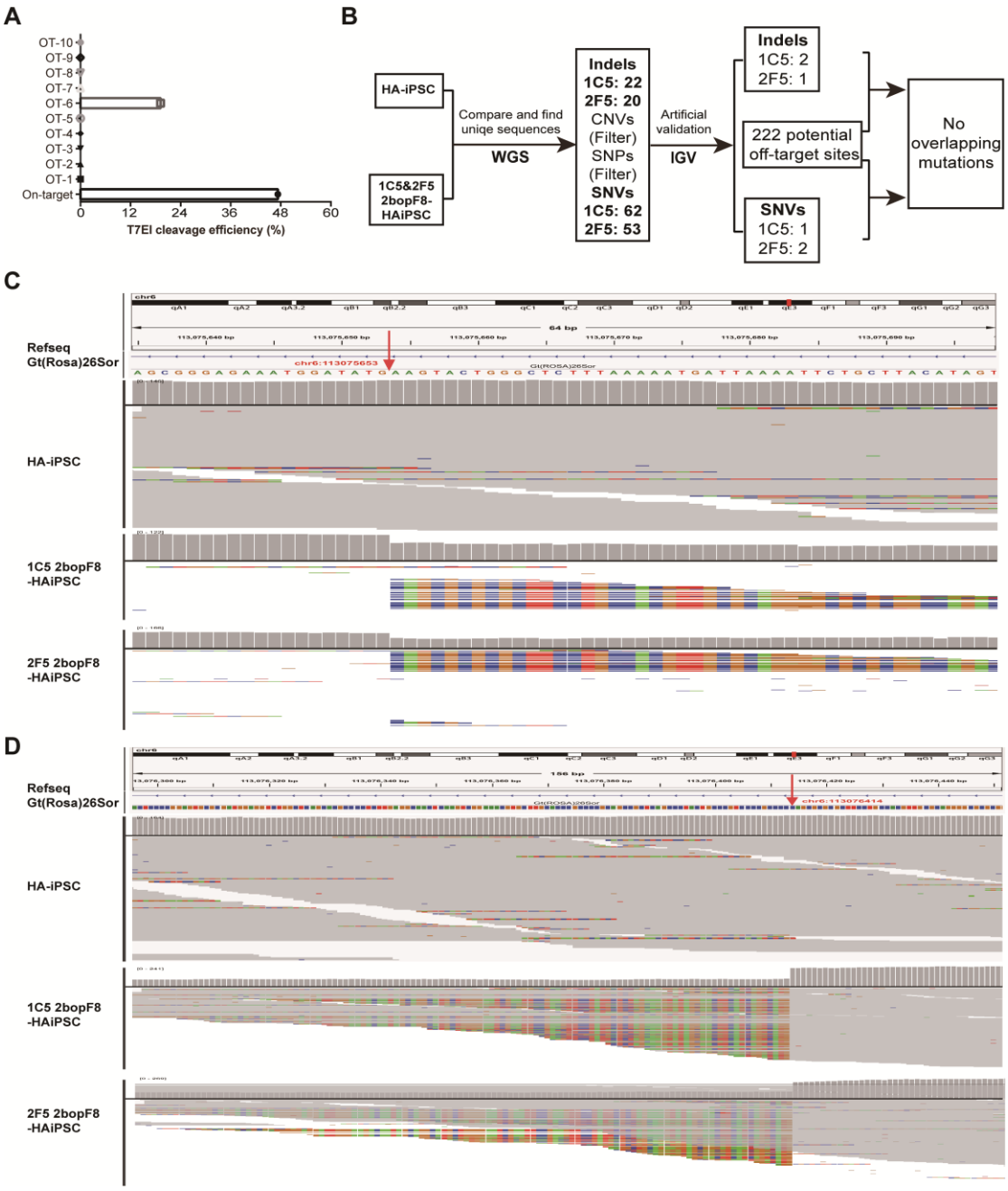

Figure S4. Whole genome sequencing for on-target and off-target analysis of iPSCs genome after genome editing.

(A) On- and off-target editing efficiency of PX330-Cas9/sgRNA-1 that targets the mouse Rosa26 locus in 2bopF8-HAiPSC clones. (B) Flow chart of off-target detection in the 2bopF8-HAiPSC clones. Using the CRISPR sgRNA design website, we found 222 potential off-target sites in the genome (Table S3). Meanwhile, we detected small insertions/deletions (indels) and single nucleotide variations (SNVs) and little mutations in genome-edited 1C5 and

2F5 clones (Table S5). Through comparison of potential off-target sites predicted by bioinformatics, we did not find any overlapping mutations. (C) The left part of the integrated breakpoint in the Rosa26 locus detected and visualized by IGV. The red arrow indicates the upper integrated site in chromosome 6:113075653. (D) The right part of integrated breakpoint in the Rosa26 locus detected and alignment by IGV. The red arrow also indicates the lower integrated site in chromosome 6:113076414.

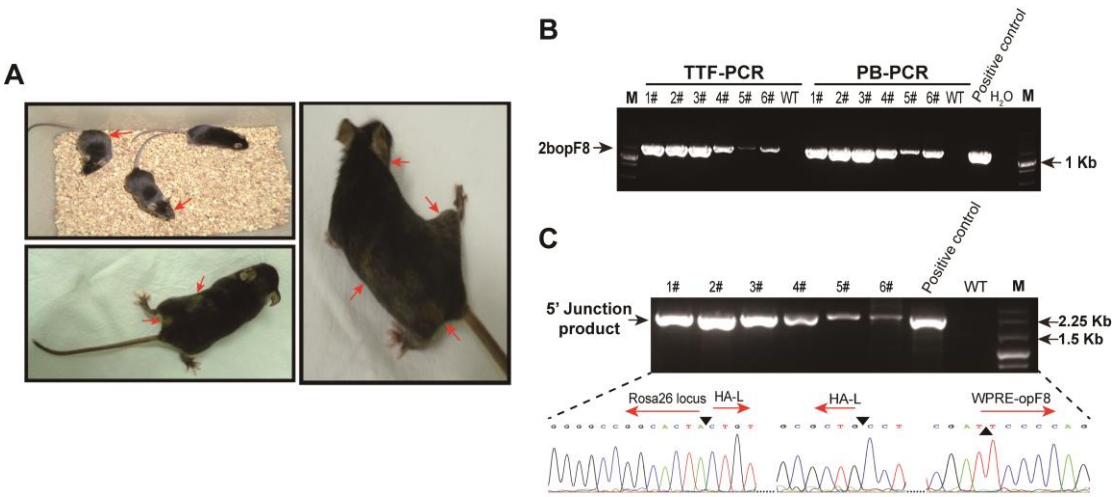

Figure S5. The coat color and molecular characters of 2bopF8-HAiPSC-derived chimeric mice.

(A) Chimeric mice (2N) produced from blastocyst injection with 2bopF8-HAiPSCs. Since the blastocysts were from C57BL/6 mouse strain and the iPSC clones were of S129 genetic background, the coat color of the chimeric mice should be the mixture of black and agouti, as indicated by the red arrows. (B) PCR analysis of 2bopF8 in chimeric mice. 2bopF8 was demonstrated in tail-tip fibroblasts (TTF) and peripheral blood cells (PBCs), confirming the existence of 2bopF8-HAiPSC-derived cells. (C) Junction PCR analysis of the integration of 2bopF8 in PBCs. PCR and subsequent sequencing results further verified the involvement of 2bopF8-HAiPSCs in the hematopoiesis of chimeras.

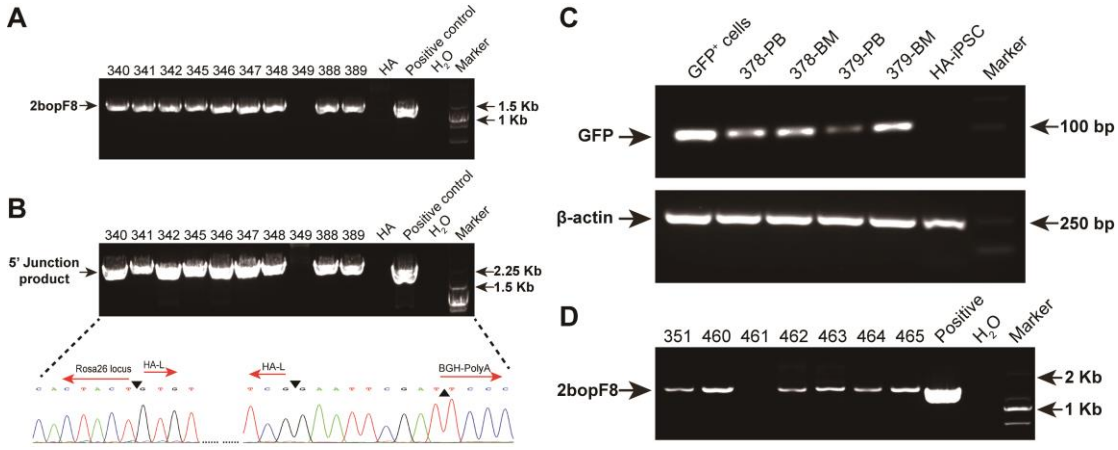

Figure S6. 2bopF8 was detected in PBC of recipients after receiving hematopoietic stem and progenitor cells (HSPCs) from chimeric mice and teratoma.

(A) 2bopF8 was detected in PBC DNA of HSPC transplantation (HSCT) recipient mice receiving HSPCs of chimeric mice except for No.349. (B) Junction PCR and sequencing analysis indicated the insertion of 2bopF8 into the Rosa26 site of PBC DNA of the chimeric mouse HSCT recipients. (C) GFP mRNA was found by RT-PCR in PB and bone marrow (BM) cells of teratoma HSCT recipients. (D) The targeted integration of the 2bopF8 cassette was detected in the PBC DNA of teratoma HSCT recipient mice at week 6.

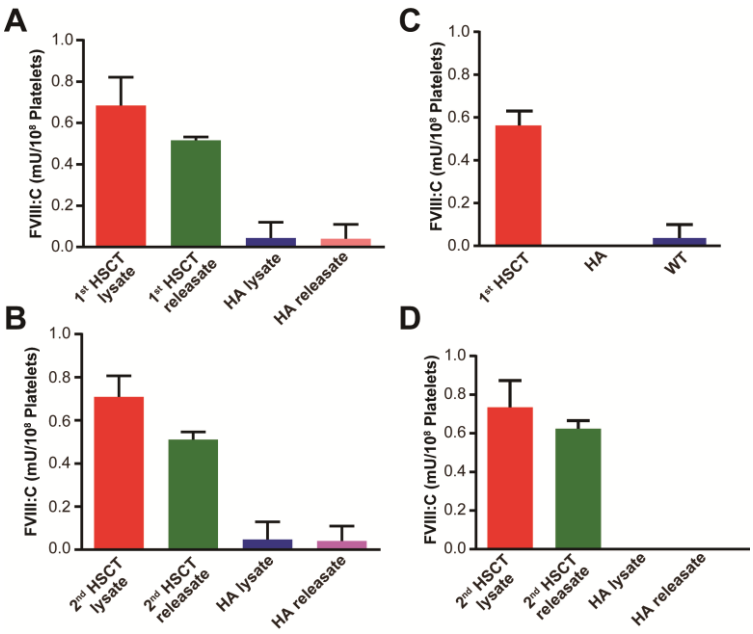

Figure S7. Quantitative evaluation of FVIII:C levels in the platelet releasates of HSCT recipient mice.

(A) FVIII:C level in the platelet releasates of the first HSCT recipient mice receiving chimeric mice HSPCs (n = 5). (B) Quantitative evaluation of FVIII:C levels in platelet releasates of the second HSCT mice (n = 6), and the FVIII:C was 0.51 ± 0.03 mU/10^8 platelets after platelet stimulation at week 12. (C) FVIII:C levels in the platelet releasates was 0.56 ± 0.06 mU/10^8 platelets of the teratoma-based first HSCT recipient mice at week 16. (D) Quantitative evaluation of FVIII:C in the platelet releasates of the second HSCT mice (n = 8), and the FVIII:C was 0.62 ± 0.04 mU/10^8 platelets at week 16.

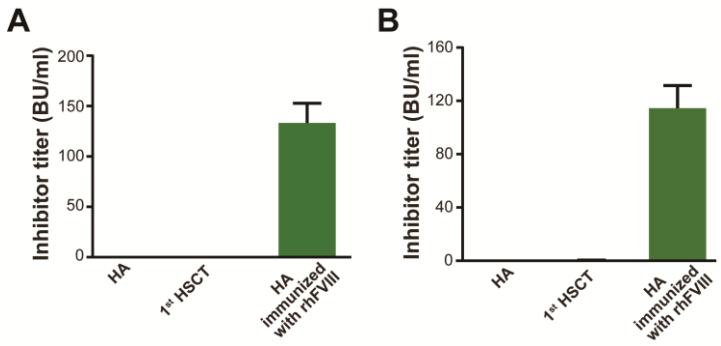

Figure S8. No FVIII inhibitor detected in the plasma of HSCT recipients.

(A) No inhibitor was found in the first recipient mice receiving chimeric mouse HSPCs (n = 5). (B) No inhibitor was found in the first recipient mice receiving teratoma-derived HSPCs (n = 5). HA mice immunized with rhFVIII (n = 3) was used as positive control.

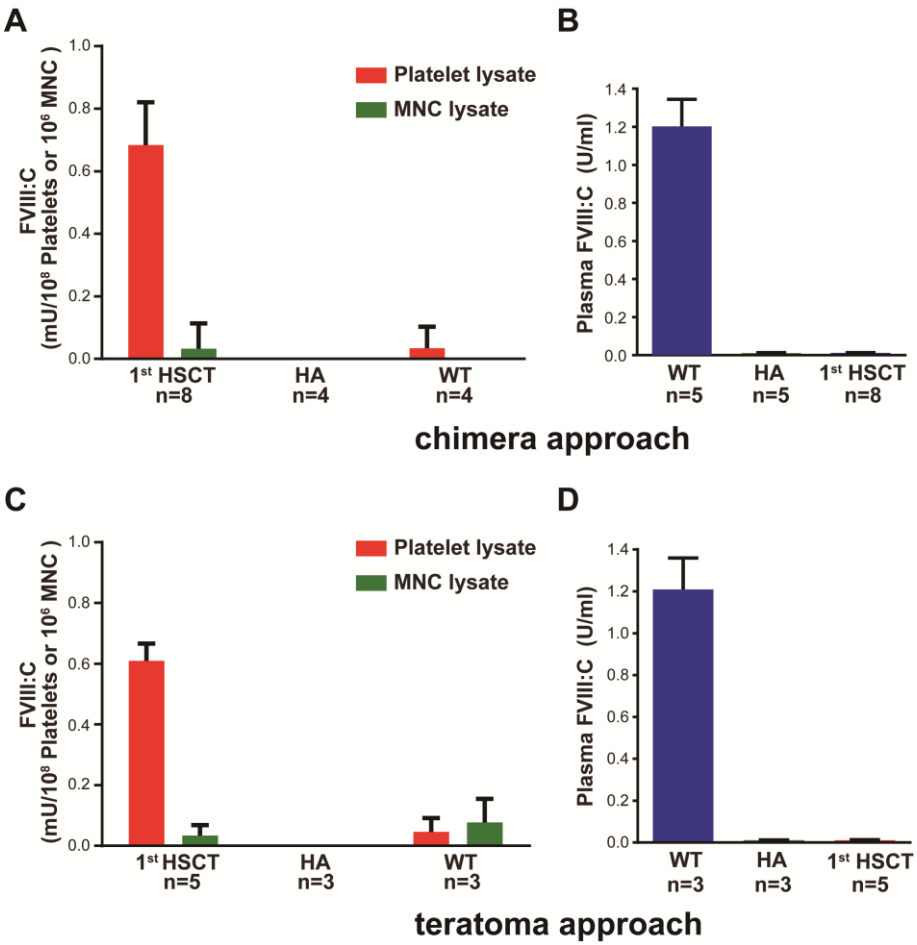

Figure S9. Evaluation the specificity of FVIII expression in blood of HSCT recipients.

(A) Quantitative evaluation of FVIII:C levels in mouse mononuclear cell (MNC) lysates from recipients after transplantation with chimera BM HSPCs. No FVIII:C was detected in MNCs of the mice, while it was only detected in platelet lysates of HSCT mice (n = 8). (B) No FVIII:C was detected in the plasma of HSCT recipients receiving chimera BM HSPCs (n = 8). (C) No FVIII:C was detected in MNCs of the recipient mice receiving teratoma-derived HSPCs (n = 5). (D) No FVIII:C was detected in plasma of the recipient mice receiving teratoma-derived HSPCs (n = 5).

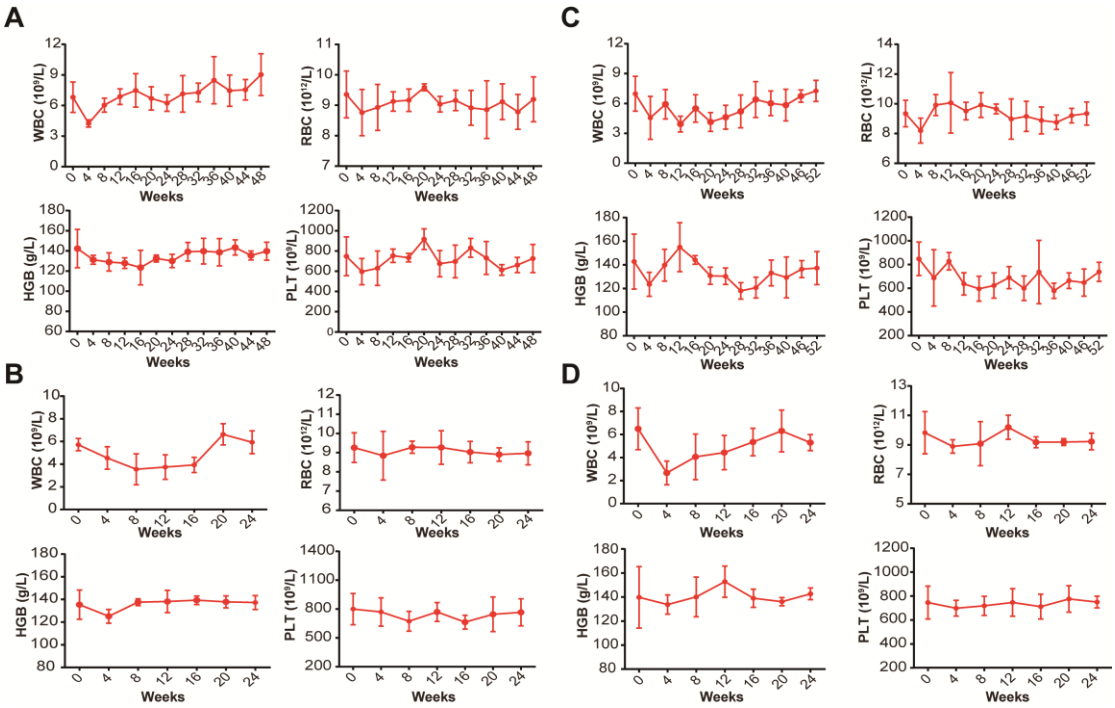

Figure S10. PBC counts in HSCT recipient mice.

(A) PBC counts was monitored for near one year in first recipients after transplantation with chimera BM HSPCs. (B) PBC counts was measured for 24 weeks in secondary HSCT mice with chimera BM HSPCs. (C) PBC counts was monitored for 52 weeks in first recipients after transplantation with teratoma-derived HSPCs. (D) PBC counts was measured for 24 weeks in secondary recipients after transplantation with teratoma-derived HSPCs. WBC, white blood cells; RBC, red blood cells; HGB, hemoglobin; PLT, platelets. Mean ± SD values are shown.

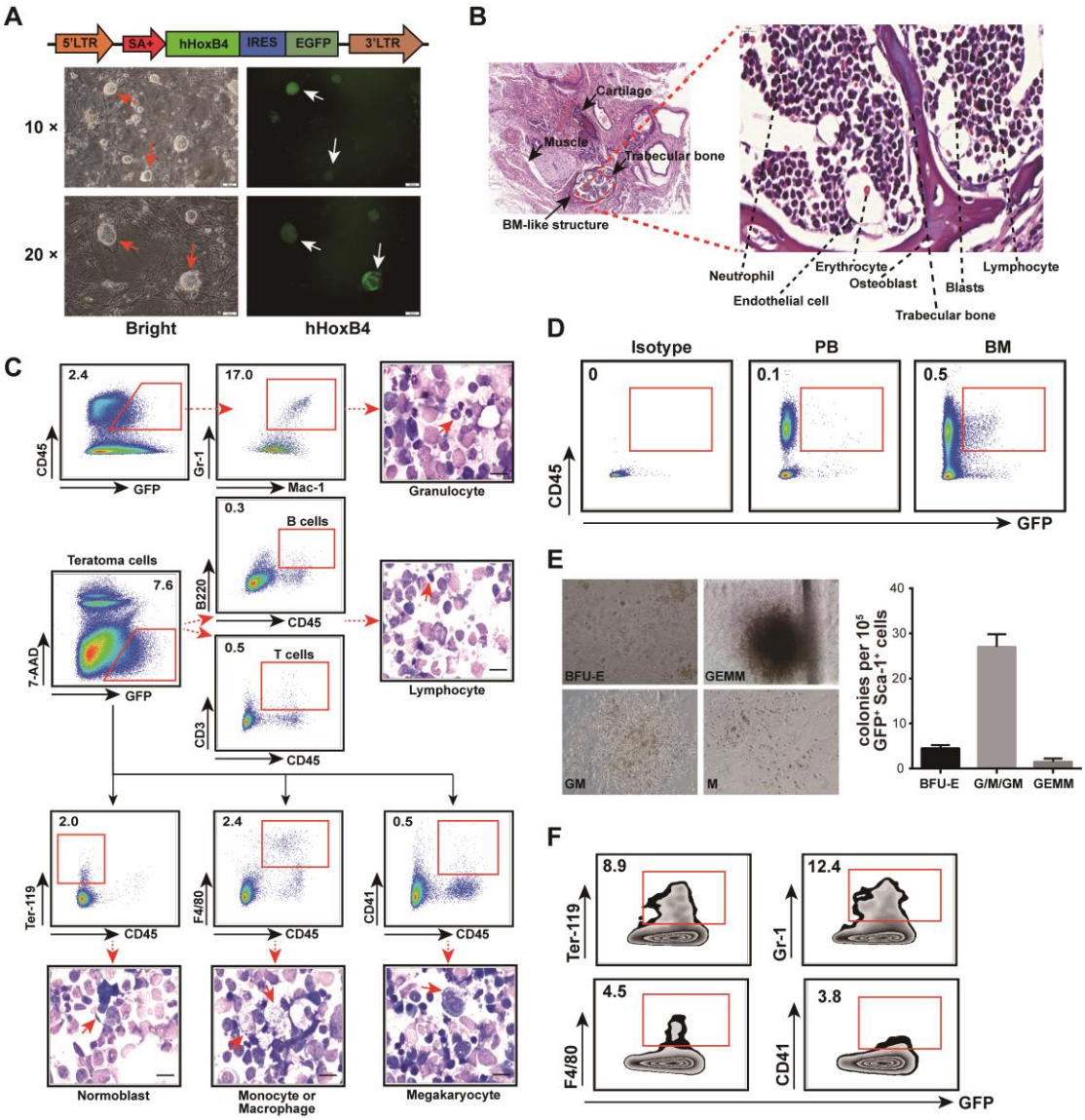

Figure S11. 2bopF8-HAiPSC-derived HSPCs from *in vivo* teratoma formation. (A) 2bopF8-HAiPSCs transduced by hHoxB4-GFP-retrovirus were sorted for GFP+ cells for further application. The upper graph represents the structure of the hHoxb4-retrovirus construct. The morphology of iPSCs in different fields and magnifications were selected; the white arrows indicate the GFP-positive iPSCs. Scale bar, upper 100 μm, lower 50 μm. (B) Teratoma section stained with HE showed typical teratoma BM–like structures. Trabecular bone, cartilage, and bone marrow were clearly visualized. Scale bar, 100 μm. Magnified field in the right indicates blood elements including neutrophils, lymphocytes, megakaryocytes (MK), and other types of cells in BM–like island. Scale bar, 10 μm. (C) FACS analysis reveals the presence of mature blood

cells, such as myeloid cells, B, T cells, erythroid cells and megakaryocytes in the GFP^+ $CD45^+$ teratoma cells. The sorted cells were stained with Giemsa for morphology validation. The percentage of each population is the indication of a representative teratoma derived by co-injection of iPSCs with OP9 cells. Scale bar, 25 μm. (D) GFP^+ $CD45^+$ blood cells were detected in PB and BM of teratoma bearing mice. (E) Colony forming cell (CFC) assay revealed the capability of GFP^+ $Sca\text{-}1^+$ cells to grow granulocyte-macrophage (GM) and macrophage (M) colonies. Few erythroids (BFU-E) and granulocytes as well as erythroids, macrophages, and megakaryocyte (GEMM) colonies were detected. (F) Flow cytometric analysis of colony forming cells from seeded teratoma-derived GFP^+ $Sca\text{-}1^+$ cells at day 13. The results showed terminally differentiated hematopoietic lineage cells, such as erythrocytes, myeloid cells, monocytes, macrophages, and megakaryocytes.

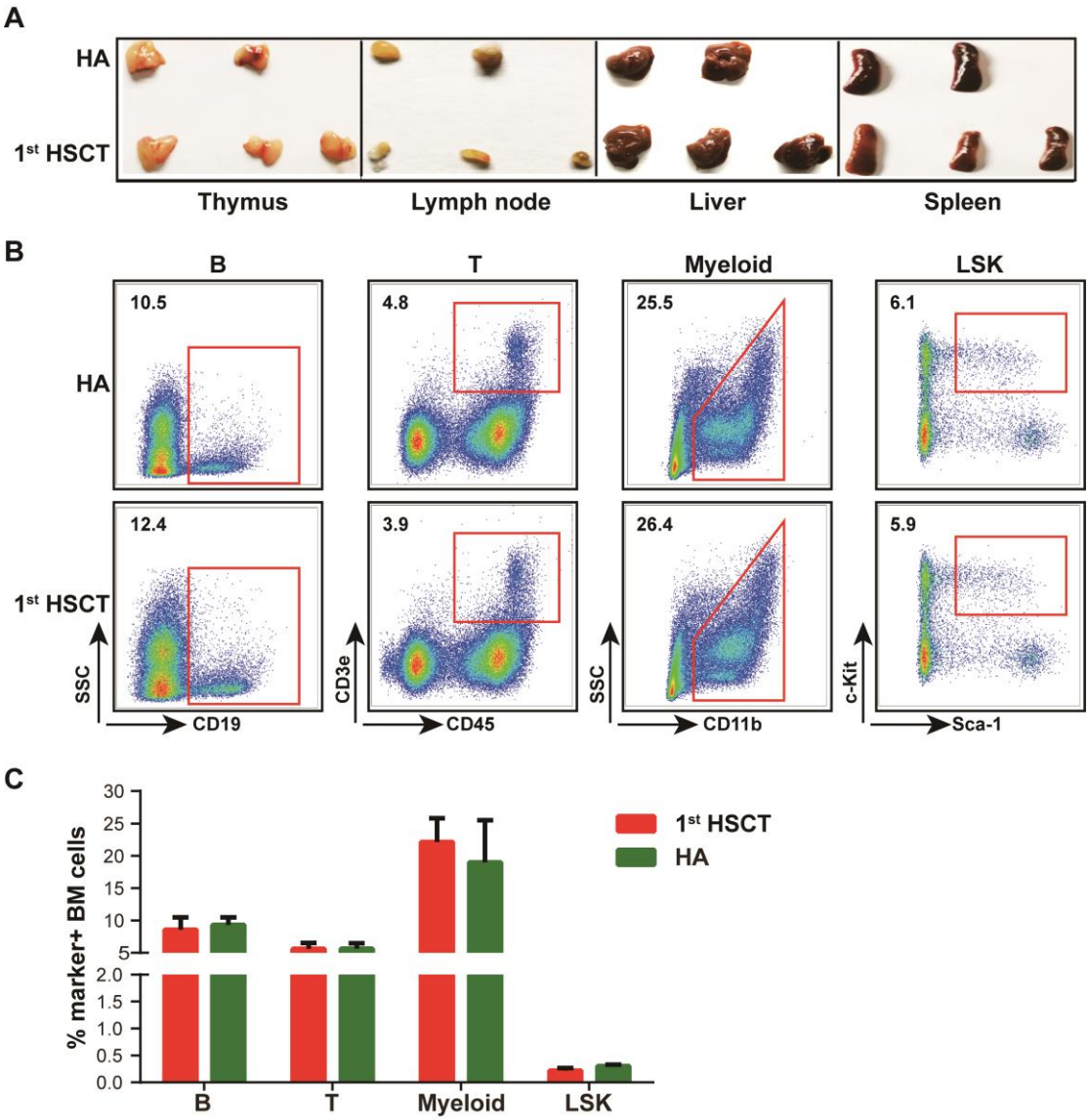

Figure S12. Characterization of organs and cells of HSCT recipient mice 52 weeks after transplanting teratoma-derived HSPCs.

(A) Comparison of the representative morphology of thymus, lymph nodes, liver, and spleen samples between the first HSCT recipients and HA control. (B) Representative flow cytometry plots showing the portion of B, T, myeloid, and HSPC lineages in BM of transplanted mice. (C) Cellular composition in bone marrow at week 52 after transplantation for data shown in B, and there is no significant differences between them.

Supplementary Tables

Table S1. The primers used for PCR, RT-PCR, qPCR.

Name	Primer sequence (5'-3')
F8KOP1/2	Forward: GAGACAGTAAACTTAGGGAAAT Reverse: ACTAGTGAGACGTGCTACTTCC
F8KOP3/4	Forward: CTGACCGCTTCCTCGTGCTT Reverse: CCAGAAGCCATTCCAAGAGG
F8KOP5/6	Forward: CACTTGTAAGAGTTTGGGGATG Reverse: GTAATCTGGAAATCACGGATGC
Oct4RT	Forward: TCTTTCCACCAGGCCCCCGGCTC Reverse: TGCGGGCGGACATGGGGAGATCC
Sox2RT	Forward: TAGAGCATGACTCCGGGCGATGA Reverse: TTGCCTTAAACAAGACCACGAAA
NanogRT	Forward: CAGGTGTTTGAGGGTAGCTC Reverse: CGGTTCATCATGGTACAGTC
Fgf4RT	Forward: CGTGGTGAGCATCTTCGGAGTGG Reverse: CCTTCTTGGTCCGCCCGTTCTTA
Rex1RT	Forward: CCCTCGACAGACTGACCCTAA Reverse: TCGGGGCTAATCTCACTTTCAT
GAPDHRT	Forward: AGGTCGGTGTGAACGGATTTG Reverse: TGTAGACCATGTAGTTGAGGTCA
T7EP	Forward: GAAGGAGCGAGGGCTCAGTTGG Reverse: ATACTCCGAGGCGGATCACAAGC
Cas9TIsg1-5J	Forward: GAGGTGGGGGTGGCGAAGGTAATG Reverse: CTGGGGATGCGGTGGGCTCTATGG
Cas9TIsg1-3J	Forward: CAGTGCTGGGGACAGGGTGGTGA Reverse: AGTGTTGAGGGCAATCTGGGAAGG
Cas9WTP	Forward: TGGCGTGTTTTGGTTGGCGTAAGG Reverse: AAAACCGAAAATCTGTGGGAAGTC
Cas9TIP	Forward: TGGCGTGTTTTGGTTGGCGTAAGG Reverse: GACAGCAGCGGCATCAAGCACAAC
mChimopf8P	Forward: GGTGCTGTTGCCCCGGTAGGTCTG Reverse: GCCCCCACGTGCTGCGGAATAG
3FHoxB4GP	Forward: GGTGCTGTTGCCCCGGTAGGTCTG Reverse: GCCCCCACGTGCTGCGGAATAG
mBGFPRT	Forward: ACTACCTGAGCACCCAGTCC Reverse: CTTGTACAGCTCGTCCATGC
mactinRT	Forward: GTGACGTTGACATCCGTAAAGA Reverse: GCCGGACTCATCGTACTCC
TAHDopf8qRT	Forward: CAGAACGGCAAAGTGAAAGTG

	Reverse: ACTTCCATTCTCAGGGCAATC Probe: FAM-AGATACCTGCGGATCCACCCTCA-TAMRA
mApoBqRT	Forward: CACGTGGGCTCCAGCATT Reverse: TCACCAGTCATTTCTGCCTTTG Probe: Cy5-CCAATGGTCGGGCACTGCTCAA-BHQ-3
Sg1OT-1P	Forward: TCCTAAGTGCTGGGAATAAA Reverse: TAAGCCTCGTGTGAGAAAAT
Sg1OT-2P	Forward: TTCCACTGTGAGTCCTGCTT Reverse: CTAAATCTTTGACCGCTGAT
Sg1OT-3P	Forward: AAGTAGGCTCTAATGCCAGTG Reverse: GAGGCTTCAAGGAACCAGTC
Sg1OT-4P	Forward: ATGGCATCTCAAGATTCTCC Reverse: ATCAGGCTCCCCTCCAACTC
Sg1OT-5P	Forward: AAACAAAGACCCAGCCACCA Reverse: GGATTCTCAGCCTCATACCC
Sg1OT-6P	Forward: AATCCCAGTGTCAAACATCC Reverse: TCTTCAGGCTTGGTCATCTC
Sg1OT-7P	Forward: GTTGTTGGAAGGAGCAAATGAAT Reverse: AGATAGCCCCCAAGAACAGAT
Sg1OT-8P	Forward: AGACTATTCAGCGTGTTCCC Reverse: CTCACTGCGGTTCAGTTTTC
Sg1OT-9P	Forward: CCCAACTCTACCGCCAGTATCTG Reverse: GGGACACGCACTTGGAACCTA
Sg1OT-10P	Forward: TCCCCAAACCTAATTGCGTTCA Reverse: GGGCCGTGGTGTGGCTTACT

Table S2. The sequence of sgRNAs used in the study.

Target locus	sgRNA	Site	Sequence (5'-3')	PAM sequence
Rosa26	sgRNA-1	intron 1	GAGTGTTGCAATACCTTTCT	NGG
	sgRNA-2	intron 1	GGCAGGCTTAAAGGCTAACC	TGG

Table S3. The potential off-target sites of sgRNA-1 were predicted by CRISPR online tool.

Table S4. The details of WGS results.

Table S5. The off-target sites of 2bopF8-HAiPSC clones detected by WGS.

Clone	Chromosome	Start	End	Reference	Alteration	Func.refGene	Depth	VAF
1C5	chr11	48752974	48752974	G	A	intergenic	227	0.03965
	chr4	103266936	103266941	GAAACG	A	intronic	204	0.03922
	chr6	73619468	73619483	GTTCATATTGTTGCAA	-	intergenic	140	0.02143
2F5	chr2	85621210	85621211	TT	AC	intergenic	159	0.04403
	chr6	72135994	72135994	C	T	intronic	231	0.02597
	chrX	95100590	95100590	G	A	intronic	125	0.016

VAF: Variant allele frequency.

Table S6. A summary of the blastocyst injection for generating chimera.

Clone name		Number of blastocyst	Number of born mice	Number of chimeras
2bopF8-HAiPSC	2F5	20	0	0
	1C5	30	5	3
	1G5	20	0	0
	2F5	20	0	0
	1C5	30	7	3

The genome-edited 2bopF8-HAiPSC clones were tested for blastocyst injection. Number of born mice and chimeras are shown. Three chimeric mice had the chimerism higher than 50 percent.

Supplemental materials and methods

Vector construction and FVIII codon optimization. The GPαIIb promoter and hHoxB4 retroviral vector were obtained from David A. Wilcox and Mitsujiro Osawa, respectively. FVIII codon optimization was performed by GeneArt® (Thermo Fisher). A codon-optimized B-domain deleted (BDD) FVIII cDNA (opF8) was synthesized, in which the B-domain was substituted by a 14-amino acid SQ sequence[1] (*Figure S1A*). The opF8 and the wild-type (WT) counterpart *F8* were cloned into the vector PCI-neo to generate PCI-opF8 and PCI-F8, respectively. These cassettes were subcloned into PCI-2bF9, in place of *F9*, to place the cassettes under control of the αIIb promoter, and named them as PCI-2bopF8 and PCI-2bF8, respectively. TetO-FUW-OSKM plasmid containing the tet-inducible tandem expression cassette for murine *Oct4*, *Sox2*, *Klf4*, and *c-Myc* was obtained from Addgene. The sgRNA sequences (sgRNA-1/2) targeting the intron 1 of the mouse Rosa26 locus were designed and subcloned into the PX330 vector as Cas9/sgRNA-1/2 by using previously reported method.[2] The donor plasmid was constructed by insertion of a 2.0 kb left homology arm and a 4.7 kb right homology arm of the Rosa26 targeting site into the pBR322 vector (Takara). The 2bopF8 cassette was inserted between the two homology arms in reverse direction.

Mice. HA mouse is a *F8* knockout mouse made by deleting exons 16−19 from the *F8* gene (Shanghai Research Center for Model Organisms),[3] and the phenotypes are the same as previously reported mouse models.[4] NOD-SCID mice (SLAC Laboratory Animal, Shanghai) and all other mice were maintained under SPF conditions and permitted for use by Ruijin Hospital Ethics Committee, Shanghai Jiao Tong University School of Medicine. Six- to 10-week old male mice were chosen as recipients for HSCT.

Cell transfection. Cells were transiently transfected with liposome reagent according to the manufacturer's instructions. PCI-opF8, PCI-F8, and PCI-neo were transfected into 293T cells with Lipofectamine 2000 (Invitrogen). After 6

hours, the medium was changed to Opti-MEM (Gibco). The supernatant was collected 48 and 72 hours after transfection for FVIII:C test. For Dami cell transfection, PCI-2bopF8, PCI-2bF8, PCI-opF8, PCI-F8, and PCI-neo were used. The medium was changed to IMDM supplemented with 10% horse serum (Hyclone) 6 hours after the transfection. The medium was then replaced with Opti-MEM added with 100 nm/L phorbol-12-myristate-13- acetate (PMA) and cultured for 24 hours. After 48 hours of culture, the cells were collected for lysing. 3T3 cells were transfected with PX330 plasmid with or without donor plasmid using Polyjet (SignaGen Laboratories). After 48 hours, cells were harvested for DNA extraction and analysis.

Derivation, maintenance, and identification of HA mouse iPS cell lines (HA-iPSCs). HA-iPSCs were reprogramed from neonatal HA mouse tail tip fibroblast (TTF). We utilized the lentiviral vector based doxycycline inducible OSKM reprogramming system as previously described.[5] The mESC-like colonies were manually collected into a new dish precoated with irradiated mouse embryonic fibroblasts (MEFs) for further expansion and characterization. RNA extraction, RT-PCR, immunofluorescence staining, embryoid bodies (EB) *in vitro* differentiation, and teratoma formation were performed as previously described for iPSCs characterization.[6]

CRISPR/Cas9-mediated genome editing of HA-iPSCs. HA-iPSCs were transfected with Cas9/sgRNA-1 and the donor plasmid by Xfect™ mESC Transfection Reagent (Clontech). Monoclonal cell populations were isolated by limiting dilution, and 2bopF8-positive clones (2bopF8-HAiPSCs) were screened by junction PCR using primers that bind outside of the homology arms in the targeted Rosa26 locus and within the recombined 2bopF8 cassette.

FVIII activity and antigen assays. Mouse blood was collected from the retro-orbital. Plasma and platelet collection, platelet lysate preparation, and platelet activation were performed as previously described.[7] FVIII:C was assessed using a FVIII chromogenic assay kit (HYPHEN Biomed) following

the manufacturer's instructions. Human FVIII antigen was determined through a human FVIII-specific sandwich ELISA protocol.[8]

Western blot analysis of FVIII. The supernatant was collected 48 hours after transfection of 293T cells and concentrated using Pierce® concentrator (Millipore). After treatment with 100 μM DTT, the reduced samples were subjected to SDS-PAGE. The PVDF membrane was blocked for 2.5 hours and incubated with a sheep anti-human factor VIII polyclonal antibody (Affinity biologicals) at 1:1,000 dilution for 8 hours at 4 °C. The blot was then incubated with donkey anti-sheep IgG-HRP (Santa Cruz) at 1:3,000 dilution for 1 hour. The blot was exposed to Immobilon™ Western Chemiluminescent Substrate (Millipore) for detection.

FVIII inhibitor assay. FVIII inhibitors were determined using a modified Bethesda assay.[9] Sequential dilutions of mouse plasma were incubated with equal volumes of 1 U/mL recombinant FVIII (rhFVIII, Baxter) at 37 °C for 2 hours. Residual FVIII:C was measured through chromogenic assay. Bethesda units were defined by diluting the blood plasma until 50% of the initial FVIII activity was neutralized. Plasma from HA mice immunized with rhFVIII was used as positive control.

T7EI-based mutation detection. Genomic mutations induced by CRISPR/ Cas9 were detected using T7 Endonuclease I (NEB).[10] The PCR fragments were amplified with KOD-Plus DNA polymerase (TOYOBO). Equal amounts of test and control PCR products were denatured and re-annealed using a thermal cycler and treated with T7EI. The DNA fragments were analyzed by agarose gel electrophoresis. The oligonucleotide primer sequences used to detect mutations are described in Table S1.

Whole genome sequencing (WGS). Genomic DNA from different samples (untreated HA-iPSCs and clones 1C5 and 2F5) was extracted and subjected to quality assessment. Libraries for WGS were constructed using TruSeq Nano DNA Library Prep Kit (Illumina) and sequenced at an average genome-wide coverage of 60 × by using 150 bp mate-paired reads. WGS data were

generated by Illumina HiSeq X Ten platform (CloudHealth, Shanghai), and bioinformatics analysis was carried out by our bioinformatics group. Additional detailed information is listed in supplementary methods.

On-target and off-target analyses. Paired-end reads (FASTQ format) were aligned to the mouse reference genome (mm10) by using BWA[11] to produce BAM file and ordered by the reads name. For on-target analysis, according to the flag in the BAM file, the reads with one end aligned to the reference genome and the other end without alignment to the reference genome were extracted. These extracted reads were aligned with the integration sequence. The reads were then extracted from one end on the reference genome and the other end on the reads of the integration sequence based on CIGAR (Compact Idiosyncratic Gapped Alignment Report) values of SAM file. The homologous regions were removed. Investigations were performed to delete false positive sites via IGV tool.[12]

Off-target prediction was implemented using the CRISPR design website (http://crispr.mit.edu/) based on mismatching with sgRNA-1 sequence by up to four nucleotides in the genome. Meanwhile, off-target analysis was carried out base on BAM file as mentioned above. Sambamba software[13] was applied to remove PCR duplications and obtain the reverse complement sequence by using sgRNA-1 and PAM sequences. Given that the mutation types were insertion/deletions (indels) and single nucleotide variations (SNVs) induced by CRISPR/Cas9 based on its mechanism, we filtered other mutation types. The homologous region of the reverse complement sequence on mm10 was obtained using BLAST tool. Freebayes[14] was invoked to detect SNVs and indels in the homologous region with an interval up and down 100 bp between HA-iPSCs control and 1C5 & 2F5 samples. The raw data were filtered by IGV to eliminate potential false-positive results. Finally, the processed off-target sites were mapped with the bioinformatics predicted sites to exclude false-positive results.

Vector copy number analysis. Genomic DNA was extracted from white blood cells. The copy number of 2bopF8 integrated cassette was measured using quantitative RT-PCR with synthesis Taqman probe (Shanghai Sangon Biotech) on ABIPRISM 7500 and normalized by mouse ApoB endogenous gene.[15] The primers and probes are listed in Table S1.

PCR and RT-PCR analysis. Genomic DNA was extracted from PB or cell lines. The PCR fragments were amplified with KOD FX Neo DNA polymerase (TOYOBO). RNA was extracted using TRIzol reagent (Invitrogen). About 0.1–1 μg of RNA for each sample was reversely transcribed using SuperScript III (Invitrogen). Mouse β-actin was set as endogenous control. All the primers used in this study are shown in Table S1.

Production of chimeric mice. Blastocyst injection was carried out by Shanghai Research Center for Model Organisms. Fifteen 2bopF8-HAiPSCs cells were injected into C57BL/6-derived blastocysts. After the injection, the aggregated blastocysts were cultured in DMEM for 1 hour and then transplanted into the uterine horn of 2.5-dpc pseudopregnant mice. After birth, the newborn F0 mice were regarded as chimeras for screening.

Teratoma formation and cell preparation. In brief, 1×10^6 OP9 stroma cells and 2×10^6 2bopF8-HAiPSCs were injected intramuscularly into NOD-SCID recipient mice with the addition of cytokines SCF and TPO (200 ng each, PeproTech) per injection. After 4 to 6 weeks, teratomas were harvested, sliced in smaller pieces, incubated, and vibrated for 1 hour at 37°C in a solution of collagenase IV/Dispase (Roche). Then cells were manually disaggregated and treated with DNase I (StemCell) for 15 minutes at room temperature. The cell suspension was filtered through a 70 μM cell strainer and labeled with appropriate antibodies for flow cytometer analysis or fluorescence-activated cell sorting (FACS).

Flow cytometry analysis and FACS. Cells were suspended in FACS buffer (DPBS containing 1% FBS) and stained with fluorochrome-conjugated antibodies, such as CD45-BV421 or APC, Sca-1-PE, and c-Kit-APC. Flow

cytometric data were collected using an LSRFortessa^{TM} X-20 flow cytometer (Becton Dickinson) and analyzed with FlowJo software (TreeStar). The cells were sorted by FACSAria III (Becton Dickinson) into 1× DPBS buffer.

Colony-forming cell assay. The GFP$^+$ Sca-1$^+$ cells were sorted from teratomas and plated into methylcellulose medium (GF M3434; StemCell Technologies) according to the manufacturer's instructions. The mixture was then added to 35 mm dishes and maintained for 12 to 14 days in a humidified chamber. When macroscopic colonies were visible, the colonies were scored manually under the microscope.

HE and Giemsa staining. Teratomas were harvested, fixed overnight with 10% formaldehyde, embedded in paraffin, and sectioned for hematoxylin and eosin staining. The histological findings were assessed by light microscopy of the stained sections. The sorted cells were subject to Wright-Giemsa staining after cytospin preparation for routine cell morphology.

Hydrodynamic tail vein injection. Plasmids PCI-opF8, PCI-F8, and PCI-neo were extracted with endofree plasmid mega kit (Qiagen). A total of 200 μg of plasmids in 2 mL of 0.9% NaCl solution was injected into the tail vein of HA mice within 6−8 s.[16] After 24 hours, plasma was collected and subjected to FVIII:C assay.

HSCT. Sca-1$^+$ cells from bone marrow (BM) and teratoma were sorted using anti-mouse Sca-1 microbeads (Miltenyi) in accordance with the manufacturer's instructions, and transplanted into lethally irradiated (10 Gy) male HA mice. BM Sca-1$^+$ cells from first recipient mice 16 weeks after primary HSCT were transplanted into lethally irradiated secondary recipients.

Tail bleeding time (BT) and relative blood loss analysis. All the mice used in these experiments were at least 8 weeks of age after HSCT and anaesthetized by 2.5% avertin during the procedure. The modified BT test was carried out based on previous reports.[17] BT was monitored continuously every half an hour for 6 hours, and the clotting time was recorded. If bleeding continued more than 6 hours, then the wounded tail tip would be cauterized

and the BT was recorded as 6 hours. For the relative blood loss test, 50 μL of blood was collected before and 6 hours after the tail tips were incised. Hemoglobin (Hb) was measured using the pocH-100iv Diff veterinary counter (Sysmex). The Hb level was normalized by defining its pretest levels as 100%.[18]

Thrombelastograph® (TEG) analysis. Blood was collected, mixed with 3.8% sodium citrate at the ratio of 9:1, and transferred into Kaolin tube. About 340 μL of mixed whole blood was added into TEG disposable cup pre-added with 20 μL of 0.2 M $CaCl_2$. Clotting analysis was initiated at 37 ℃ by using TEG 5000 analyzers (Haemoscope). The reaction time (R value) was recorded as clotting time (CT).

Statistical analysis. Statistical significance was performed with GraphPad Prism 6 (two-tailed Student's *t* test) and $P<0.05$ were considered statistically significant.

References

1. Sandberg H, Almstedt A, Brandt J, et al. Structural and functional characteristics of the B-domain-deleted recombinant factor VIII protein, r-VIII SQ. Thromb Haemost. 2001;85(1):93-100.
2. Ran FA, Hsu PD, Wright J, Agarwala V, Scott DA, Zhang F. Genome engineering using the CRISPR-Cas9 system. Nat Protoc. 2013;8(11):2281-2308.
3. Kuang Y, Wang J, Lu X, et al. Generation of factor VIII gene knockout mouse by tetraploid embryo complementation technology. Zhonghua Yi Xue Yi Chuan Xue Za Zhi. 2010;27(1):1-6.
4. Bi L, Lawler AM, Antonarakis SE, High KA, Gearhart JD, Kazazian HH, Jr. Targeted disruption of the mouse factor VIII gene produces a model of haemophilia A. Nat Genet. 1995;10(1):119-121.
5. Sun M, Liao B, Tao Y, et al. Calcineurin-NFAT Signaling Controls Somatic Cell Reprogramming in a Stage-Dependent Manner. J Cell Physiol. 2016;231(5):1151-1162.
6. Li L, Sun L, Gao F, et al. Stk40 links the pluripotency factor Oct4 to the Erk/MAPK pathway and controls extraembryonic endoderm differentiation. Proc Natl Acad Sci USA. 2010;107(4):1402-1407.

7. Shi Q, Wilcox DA, Fahs SA, et al. Factor VIII ectopically targeted to platelets is therapeutic in hemophilia A with high-titer inhibitory antibodies. J Clin Invest. 2006;116(7):1974-1982.
8. Wang Q, Dong B, Firrman J, et al. Efficient production of dual recombinant adeno-associated viral vectors for factor VIII delivery. Hum Gene Ther Methods. 2014;25(4):261-268.
9. Verbruggen B, Novakova I, Wessels H, Boezeman J, van den Berg M, Mauser-Bunschoten E. The Nijmegen modification of the Bethesda assay for factor VIII:C inhibitors: improved specificity and reliability. Thromb Haemost. 1995;73(2):247-251.
10. Gundry MC, Brunetti L, Lin A, et al. Highly Efficient Genome Editing of Murine and Human Hematopoietic Progenitor Cells by CRISPR/Cas9. Cell Rep. 2016;17(5):1453-1461.
11. Li H, Durbin R. Fast and accurate short read alignment with Burrows-Wheeler transform. Bioinformatics. 2009;25(14):1754-1760.
12. Robinson JT, Thorvaldsdottir H, Winckler W, et al. Integrative genomics viewer. Nat Biotechnol. 2011;29(1):24-26.
13. Tarasov A, Vilella AJ, Cuppen E, Nijman IJ, Prins P. Sambamba: fast processing of NGS alignment formats. Bioinformatics. 2015;31(12):2032-2034.
14. Chiang C, Layer RM, Faust GG, et al. SpeedSeq: ultra-fast personal genome analysis and interpretation. Nat Methods. 2015;12(10):966-968.
15. Lizee G, Aerts JL, Gonzales MI, Chinnasamy N, Morgan RA, Topalian SL. Real-time quantitative reverse transcriptase-polymerase chain reaction as a method for determining lentiviral vector titers and measuring transgene expression. Hum Gene Ther. 2003;14(6):497-507.
16. Liu F, Song Y, Liu D. Hydrodynamics-based transfection in animals by systemic administration of plasmid DNA. Gene Ther. 1999;6(7):1258-1266.
17. Chen Y, Luo X, Schroeder JA, et al. Immune tolerance induced by platelet-targeted factor VIII gene therapy in hemophilia A mice is CD4 T cell mediated. J Thromb Haemost. 2017;15(10):1994-2004.
18. Schroeder JA, Chen Y, Fang J, Wilcox DA, Shi Q. In vivo enrichment of genetically manipulated platelets corrects the murine hemophilic phenotype and induces immune tolerance even using a low multiplicity of infection. J Thromb Haemost. 2014;12(8):1283-1293.